

## Accepted Manuscript

Potent and selective inhibitors of receptor-interacting protein kinase 1 that lack an aromatic back pocket group

Gregory L. Hamilton, Huifen Chen, Gauri Deshmukh, Charles Eigenbrot, Rina Fong, Adam Johnson, Pawan Bir Kohli, Patrick J. Lupardus, Bianca M. Liederer, Sreemathy Ramaswamy, Haowei Wang, Jian Wang, Zhaowu Xu, Yunliang Zhu, Domagoj Vucic, Snahel Patel

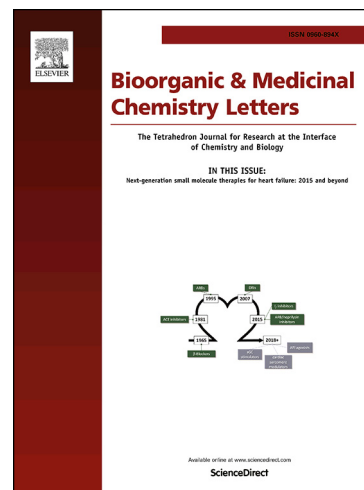
PII: S0960-894X(19)30223-9  
DOI: <https://doi.org/10.1016/j.bmcl.2019.04.014>  
Reference: BMCL 26381

To appear in: *Bioorganic & Medicinal Chemistry Letters*

Received Date: 13 February 2019  
Revised Date: 2 April 2019  
Accepted Date: 6 April 2019

Please cite this article as: Hamilton, G.L., Chen, H., Deshmukh, G., Eigenbrot, C., Fong, R., Johnson, A., Bir Kohli, P., Lupardus, P.J., Liederer, B.M., Ramaswamy, S., Wang, H., Wang, J., Xu, Z., Zhu, Y., Vucic, D., Patel, S., Potent and selective inhibitors of receptor-interacting protein kinase 1 that lack an aromatic back pocket group, *Bioorganic & Medicinal Chemistry Letters* (2019), doi: <https://doi.org/10.1016/j.bmcl.2019.04.014>

This is a PDF file of an unedited manuscript that has been accepted for publication. As a service to our customers we are providing this early version of the manuscript. The manuscript will undergo copyediting, typesetting, and review of the resulting proof before it is published in its final form. Please note that during the production process errors may be discovered which could affect the content, and all legal disclaimers that apply to the journal pertain.



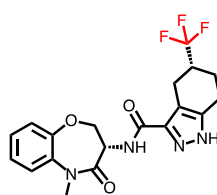
## Graphical Abstract

To create your abstract, type over the instructions in the template box below.  
Fonts or abstract dimensions should not be changed or altered.

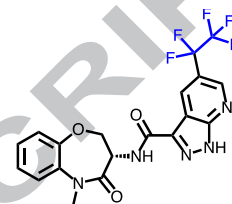
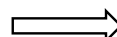
### Potent and selective inhibitors of receptor-interacting protein kinase 1 that lack an aromatic back pocket group

Gregory L. Hamilton, et al.

Leave this area blank for abstract info.



Compound **18**  
RIPK1  $K_i^{app}$  = 0.007  $\mu$ M  
HT29 cell  $EC_{50}$  = 0.028  $\mu$ M  
Rat in vivo CL = 132 mL/min/kg,  $t_{1/2}$  = 0.94 h



Compound **29**  
RIPK1  $K_i^{app}$  = 0.006  $\mu$ M  
HT29 cell  $EC_{50}$  = 0.054  $\mu$ M  
Rat in vivo CL = 7.1 mL/min/kg,  $t_{1/2}$  = 4.8 h



## Potent and selective inhibitors of receptor-interacting protein kinase 1 that lack an aromatic back pocket group

Gregory L. Hamilton<sup>a</sup>, Huifen Chen<sup>a</sup>, Gauri Deshmukh<sup>a</sup>, Charles Eigenbrot<sup>a</sup>, Rina Fong<sup>a</sup>, Adam Johnson<sup>a</sup>, Pawan Bir Kohli<sup>a</sup>, Patrick J. Lupardus<sup>a</sup>, Bianca M. Liederer<sup>a</sup>, Sreemathy Ramaswamy<sup>a</sup>, Haowei Wang<sup>b</sup>, Jian Wang<sup>b</sup>, Zhaowu Xu<sup>b</sup>, Yunliang Zhu<sup>b</sup>, Domagoj Vucic<sup>a</sup>, and Snahel Patel<sup>a,\*</sup>

<sup>a</sup> Genentech Inc., 1 DNA Way, South San Francisco, CA 94080 USA

<sup>b</sup> WuXi AppTec Co., Ltd., 288 Fute Zhong Road, Waigaoqiao Free Trade Zone, Shanghai 200131, China

### ARTICLE INFO

\* Corresponding author. Tel.: +1-650-225-4272; fax: +1-650-742-4943; e-mail: patel.snahel@gene.com

### ABSTRACT

#### Article history:

Received

Revised

Accepted

Available online

#### Keywords:

RIPK1

RIPK1 inhibitor

necroptosis

metabolic stability

pentafluoroethyl

Receptor-interacting protein kinase I (RIPK1), a key component of the cellular necroptosis pathway, has gained recognition as an important therapeutic target. Pharmacologic inhibition or genetic inactivation of RIPK1 has shown promise in animal models of disease ranging from acute ischemic conditions, chronic inflammation, and neurodegeneration. We present here a class of RIPK1 inhibitors that is distinguished by a lack of a lipophilic aromatic group present in most literature inhibitors that typically occupies a hydrophobic back pocket of the protein active site. Despite not having this ubiquitous feature of many known RIPK1 inhibitors, we were able to obtain compounds with good potency, kinase selectivity, and pharmacokinetic properties in rats. The use of the lipophilic yet metabolically stable pentafluoroethyl group was critical to balancing the potency and properties of optimized analogs

2009 Elsevier Ltd. All rights reserved.

Originally recognized as a key regulator of a form of programmed cell death termed necroptosis, receptor-interacting protein kinase 1 (RIPK1) is now appreciated for a broader role across a variety of inflammatory pathways.<sup>1–5</sup> RIPK1 has been implicated in pathologic conditions ranging from ischemic brain or kidney injury, myocardial infarction, and intestinal inflammation.<sup>6–12</sup> Accordingly, there has been a surge of interest in developing small molecule inhibitors of RIPK1 as potential therapeutics. In fact, three RIPK1 inhibitors have entered clinical trials so far (GSK'772, GSK'095, and DNL-747).<sup>1</sup>

The first published RIPK1 inhibitor, known as Nec-1 (1, Fig. 1), was disclosed in 2005 by Degterev et al.<sup>7</sup> An X-ray co-crystal structure of a refined analog Nec-1a (2) revealed that the molecule has an allosteric binding mode with the indole ring occupying a hydrophobic back pocket near the ATP-binding site.<sup>14</sup> Additionally, a carbonyl of the hydantoin ring accepts a hydrogen bond from the N–H of residue Asp-156. Because these compounds do not display the hinge-binding contacts normally present in most kinase inhibitors, they exhibit extreme kinase selectivity for RIPK1.

More recently, a number of new RIPK1 inhibitors have been discovered (Fig. 2).<sup>15–20</sup> Interestingly, these molecules all share the structural features of a lipophilic aromatic ring at one end

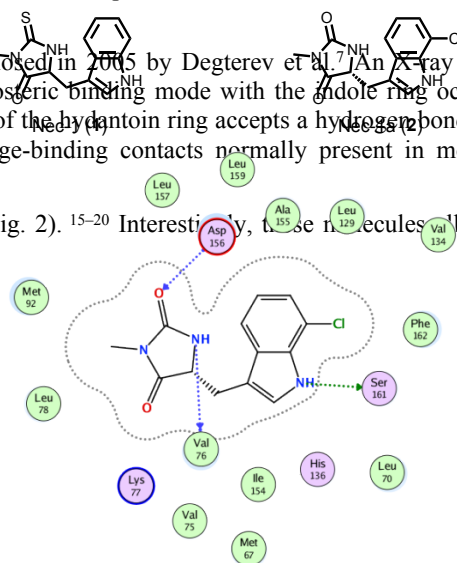


**Figure 1.** Structures of Nec-1 and Nec-1a, with a 2D representation highlighting key interactions observed in the Nec-1a-RIPK1 co-crystal structure.

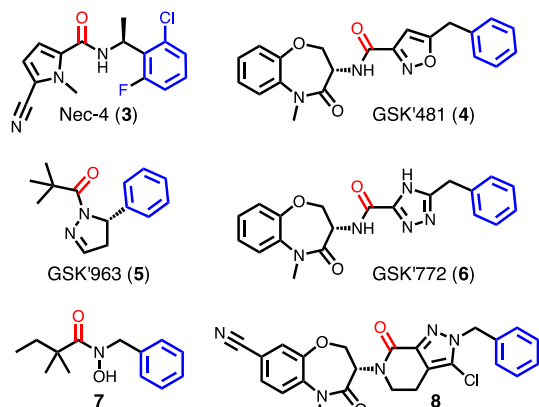


**Figure 2.** Published non-hinge binding RIPK1 inhibitors with key lipophilic aromatic ring highlighted in blue and hydrogen bond acceptor to Asp-156 highlighted in red.

linked to a carbonyl hydrogen bond acceptor by a spacer of varying length. Crystallographic studies have confirmed that the compounds have similar binding modes, with the aromatic ring always slotting into the allosteric back pocket that is exposed in the DLG-out conformation and the carbonyl making contact with the N–H of DLG's Asp156.<sup>15–20</sup>

Given the improvements in physicochemical properties that can come from reducing the number of aromatic rings, we wanted to assess whether having a lipophilic aromatic present in the enzyme back pocket was in fact an absolute requirement for potent and selective RIPK1 inhibition. We noted that previous reports had not described bicyclic heterocycles, which led us to consider tetrahydroindazole **9**. We tested compound **9** in a human RIPK1 biochemical inhibition assay as well as an HT29 human colorectal carcinoma cellular assay which tested the ability to prevent cell death induced by the combination of TNF $\alpha$ , zVAD-fmk, and BV6 (see Supplementary Material). Compound **9** showed a  $K_i^{app}$  of 3.4  $\mu$ M, which translated to reasonable ligand efficiency<sup>22</sup> and physicochemical properties as a starting point for further elaboration (LE = 0.31, cLogP = 1.7), despite lacking any sort of aromatic that could occupy the back pocket of RIPK1 (Table 1). It also demonstrated a measurable cellular  $EC_{50}$  of 15  $\mu$ M; this biochemical to cell shift in the five- to ten-fold range was typical of this chemical series. The activity of tetrahydroindazole **9** was noteworthy because the simple unsubstituted triazole **10** did not show any inhibition up to the top concentration tested. Reasoning that the saturated ring of the tetrahydroindazole might be contributing to potency by partially occupying the hydrophobic back pocket, we investigated the effect of placing small alkyl groups around the ring to hopefully probe further into the cavity. Gratifyingly, a properly oriented methyl group at the 5-position of the tetrahydroindazole (compound **11** vs. epimer **12**) rendered a remarkable improvement in potency by over two orders of magnitude. Notably, addition of alkyl groups at other positions of the ring did not furnish the same improvement, nor did fused cyclopropane rings (compounds **13–16**). Additionally, geminal substitution (**16**) resulted in a small loss of potency.

Based on the SAR and the activity of compound **11**, we hypothesized that the exocyclic methyl group was directed into the hydrophobic back pocket of the protein. Fortunately, we were able to test this hypothesis by obtaining an X-ray co-crystal structure of **11** bound to a RIPK1 construct based on the human enzyme (1–294, C34A, C127A, C233A, C240A). Fig. 3 depicts this data overlaid with the published co-crystal structure of inhibitor **4** (PDB code: 5HX6).<sup>15</sup> The protruding methyl group of **11** indeed appears to be occupying a similar (albeit smaller)

**Table 1.** Activity of various substituted heterocyclic analogs

| Compound  | R = | RIPK1<br>$K_i^{app}$ ( $\mu$ M) <sup>a</sup> | HT29 viability<br>$EC_{50}$ ( $\mu$ M) <sup>b</sup> |
|-----------|-----|--|---|
| <b>9</b>  |     | 3.4  | 15  |
| <b>10</b> |     | >10  | >20   |
| <b>11</b> |     | 0.016  | 0.13  |
| <b>12</b> |     | 0.10   | 0.40  |

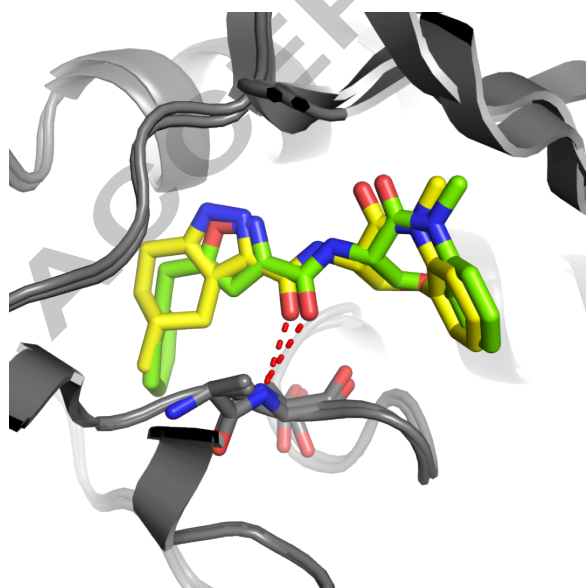
<sup>a</sup>human RIPK1 activity measured using ADP Transcreener assay; see Supplementary Material.

<sup>b</sup>HT29 human colorectal carcinoma cell viability measured after 18 h following treatment with TNF $\alpha$ , zVAD-fmk, BV6, and inhibitor; see Supplementary Material.

<sup>c</sup>Compound is a 1:1 mixture of diastereomers where no stereochemistry is specified.

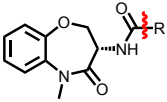
space in the pocket as the phenyl ring of **4**. The pyrazole ring of **11** also appears to be slightly displaced relative to the isoxazole of **4**, possibly to better position the methyl group into the back pocket.

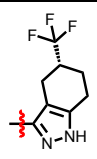
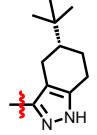
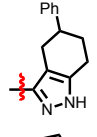
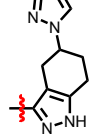
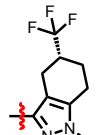
One final piece of information from the X-ray structure was that there was likely more room to grow beyond a methyl group to better fill the back pocket. Consistent with this notion, trifluoromethyl-substituted analog **18** had improved biochemical and cellular activity (Table 2). However, larger substituents such as *tert*-butyl (**19**), phenyl (**20**), or 1-pyrazolyl (**21**) were not well tolerated, which was also predicted by the co-crystal structure of **11**. Finally, methylation to mask the pyrazole N-H also led to a loss in potency, probably because it presents a steric clash with the protein.



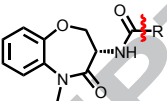
**Figure 3.** Overlay of **11** (yellow) with **4** (green) bound to RIPK1 based on X-ray crystallographic data, with H-bond to Asp156 highlighted (dashed line).

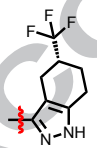
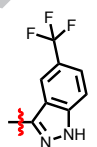
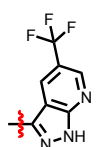
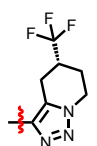
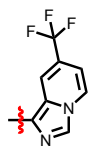
Although potent, **18** suffered from moderate liver microsomal stability that limited its potential for advancement. To address this liability, a variety of hetero-bicyclic replacements for the tetrahydroindazole were explored (Table 3). Many unsaturated and partially saturated ring systems were tolerated by the protein pocket. As might be expected, heterocycles with better distribution of polar atoms throughout the bicycle showed

**Table 2.** Activity of 5-substituted tetrahydroindazole analogs


| Compound        | R =  | RIPK1<br>$K_i^{app}$ ( $\mu$ M) | HT29 viability<br>$EC_{50}$ ( $\mu$ M) |
|-----------------|--|---------------------------------|--|
| 18              |   | 0.007                           | 0.043                                  |
| 19              |   | 0.048                           | 0.29                                   |
| 20 <sup>a</sup> |   | 0.028                           | 0.52                                   |
| 21 <sup>a</sup> |   | 0.75                            | 4.1                                    |
| 22              |  | 0.063                           | 0.5                                    |

<sup>a</sup>Compound is a 1:1 mixture of diastereomers where no stereochemistry is specified

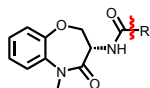
**Table 3.** Activity and liver microsomal stability of differing trifluoromethyl-substituted bicyclic cores


| Compound | R =   | RIPK1<br>$K_i^{app}$ ( $\mu$ M) | HT29 viability<br>$EC_{50}$ ( $\mu$ M) | LM $CL_{hep}$<br>(ml/min/kg)<br>human / rat <sup>a</sup> |
|----------|---|---------------------------------|--|--|
| 18       |  | 0.007                           | 0.043                                  | 8.6 / 33   |
| 23       |  | 0.005                           | 0.028                                  | 14 / 25  |
| 24       |  | 0.098                           | 0.58                                   | 9.7 / 18   |
| 25       |  | 0.064                           | 0.21                                   | 7.8 / 37   |
| 26       |  | 0.005                           | 0.012                                  | 14 / 44  |

<sup>a</sup>Predicted hepatic clearance based on 1 h time course incubation with liver microsomes (1  $\mu$ M compound, 0.5 mg/mL microsomes, 1  $\mu$ M NADPH).

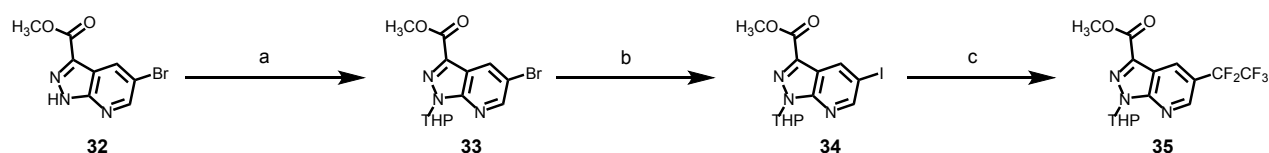
improved stability in liver microsomes. However, some of the most stable examples like **27** sacrificed too much potency to be useful. Other heterocycle permutations (**23**, **25**, and **26**) offered no improvement in microsomal stability relative to **18**, so we proceeded to examine the pharmacokinetics of **18** in an in vivo rat study. Unfortunately, the observed clearance was under predicted by the liver microsomes and in fact was greater than liver blood flow (132 mL/min/kg).<sup>23</sup> Thus **18** was not progressed any further.

The next most promising analog in terms of balancing potency and metabolic stability was 7-azaindazole **24**, although further improvements in potency were necessary. While we knew that dramatically enlarging the back pocket substituent beyond trifluoromethyl would likely be deleterious based on earlier phenyl and tert-butyl-substituted analogs **19** and **20**, we wondered whether a more modest increase in the size could improve the potency by better filling the space. Isopropyl-substituted analog **28** represented an improvement in potency of about two-fold, but at the cost of metabolic stability (Table 4). Searching for a moderately-sized yet potentially metabolically stable fragment, we considered the pentafluoroethyl moiety.<sup>24</sup> Incorporation of this piece to provide compound **29** improved the Table 4. Comparison of pentafluoroethyl examples with trifluoromethyl and isopropyl analogs



| Compound              | R = | RIPK1<br>$K_i^{app}$ ( $\mu$ M) | HT29 viability<br>$EC_{50}$ ( $\mu$ M) | LM $CL_{hep}$<br>(ml/min/kg)<br>human / rat | Kinetic<br>solubility<br>( $\mu$ M, pH 7.4) | $LogD_{7.4}$ |
|-----------------------|-----|---------------------------------|--|---|---|--------------|
| <b>24</b>             |     | 0.098                           | 0.58                                   | 9.7 / 18                                    | 59  | 3.3          |
| <b>25</b>             |     | 0.064                           | 0.21                                   | 7.8 / 37                                    | 99  | 1.5          |
| <b>27</b>             |     | 0.57                            | 2.4                                    | <3.9 / <11                                  | 160   | 1.0          |
| <b>28</b>             |     | 0.055                           | 0.39                                   | 16 / 38                                     | 3.4   | 3.5          |
| <b>29</b>             |     | 0.006                           | 0.054                                  | 11 / 14                                     | 17  | 4.1          |
| <b>30<sup>a</sup></b> |     | 0.024                           | 0.064                                  | 7.8 / 41                                    | 57.1  | 2.0          |
| <b>31</b>             |     | 0.068                           | 0.13                                   | 4.4 / 25                                    | 164   | 1.6          |

<sup>a</sup>Compound is a 1:1 mixture of diastereomers where no stereochemistry is specified.



**Scheme 1.** Synthesis of pentafluoroethyl azaindazole **29**. Reagents and conditions: (a) 3,4-dihydro-2H-pyran, pyridinium *p*-toluenesulfonate, dichloromethane, 40 °C, 6 h, 90%; (b) *trans*-*N,N'*-dimethylcyclohexane-1,2-diamine, copper(I) iodide, sodium iodide, dioxane, 110 °C, 20 h, 97%; (c) trimethylpentafluoroethylsilane, copper(I) iodide, potassium fluoride, *N,N*-dimethylformamide, 80 °C, 20 h, 42%; (d) trifluoroacetic acid, dichloromethane, rt, 2 h, 69%; (e) lithium hydroxide, tetrahydrofuran, water, rt, 10 h, 79%; (f) *N*-(3-dimethylaminopropyl)-*N'*-ethylcarbodiimide hydrochloride, 1-hydroxybenzotriazole, (S)-3-amino-5-methyl-2,3-dihydrobenzo[*b*][1,4]oxazepin-4(5H)-one (**38**), *N,N*-dimethylformamide, rt, 1 h, 52%. THP = 2-tetrahydropyranyl

cellular potency tenfold relative to the trifluoromethyl analog **24** without adversely affecting liver microsome stability. We also tried adding the pentafluoroethyl group to some of our other scaffolds and found that it consistently boosted the potency dramatically relative to trifluoromethyl substitution (matched pairs **25** vs. **30**, **27** vs. **31**). Importantly, we observed either no or only a small loss of liver microsome stability. The increase in LogD ranged from 0.5 to 0.8 relative to the trifluoromethyl matched pairs, and although the kinetic solubility did decrease somewhat, the solubility was better than the isopropyl matched pair (**28** vs. **29**).

It does not escape our attention that compound **29** contains a (hetero)aromatic group *near* the region of the inhibitor that binds in the back pocket of RIPK1, which stands in seeming contradiction to the fact that we began this study by looking for potent inhibitors that did not have a back pocket aromatic moiety. However, the crystallographic structure overlay in Fig. 3 clearly shows that the six-membered portion of the bicyclic ring system corresponding to the pyridyl portion of **29** does not occupy the same space and is oriented orthogonally to the phenyl moiety of GSK'481. Furthermore, the similar potencies of matched pair **18** (partially saturated) and **23** (aromatic) indicate that the six-membered portion of the bicycle is serving a scaffolding or linker role, whereas it is the exocyclic (fluoro)alkyl group that drives the potency by occupying the hydrophobic back pocket of RIPK1. Thus, we believe this work illuminates some heretofore unpublished structure-activity relationships of this important class of RIPK1 inhibitors.

On the basis of its RIPK1 potency and liver microsomal stability, pentafluoroethyl azaindazole **29** was progressed to an in vivo rat PK study. We were quite pleased to find that it exhibited low clearance (7.1 mL/min/kg) and moderate volume of distribution (2.8 L/kg) that translated into a 4.8-hour half-life, by far the best we had seen on this series.<sup>23</sup> Oral bioavailability was also reasonable at 63%. In addition to its other favorable attributes, **29** exhibited excellent kinase selectivity, with no level of inhibition >30% observed when tested at a single point concentration of 10 μM in a 219 human kinase panel (Thermo Fisher, see Supplementary Material). As was the case for other published inhibitors in the benzoxazepinone series, **29** showed dramatically lower potency against mouse RIPK1, with an EC<sub>50</sub> in mouse L929 cell viability assay of 11 μM.

The synthesis of **29** is outlined in Scheme 1. Commercially available methyl 5-bromo-1*H*-pyrazolo[3,4-*b*]pyridine-3-carboxylate (**32**) was protected at its N–H with a 2-tetrahydropyranyl group. Next, the bromide was swapped to a more reactive iodide in a copper-promoted reaction to set up the key pentafluoroethylation reaction. The desired fluoroalkyl cross-coupling was achieved by another Cu(I)-catalyzed reaction utilizing the pentafluoroethyl version of the Ruppert-Prakash reagent ((CH<sub>3</sub>)<sub>3</sub>SiCF<sub>2</sub>CF<sub>3</sub>). Deprotection and ester saponification completed the preparation of the acid **37**, which was coupled under EDC/HOBt conditions to amino-benzoxazepinone **38** to finish the synthesis.

Needless to say, balancing potency gains by adding lipophilicity without introducing metabolic or other liabilities is a general challenge. We believe the present case study offers an interesting example of productive use of the infrequently utilized pentafluoroethyl fragment, which is in the rare position of having moderate size and lipophilicity while being resistant to oxidative metabolism. Contemporary synthetic methods have made incorporation of this group more easily accessible by cross-coupling,<sup>25,26</sup> and many more pentafluoroethylated building blocks are now commercially available. In summary, we discovered a series of RIPK1 inhibitors that derive potency from small lipophilic alkyl groups occupying the protein back pocket, which is normally exploited by aromatic substituents in published inhibitors. Through judicious use of the pentafluoroethyl motif, we were able to find a compound with good potency and pharmacokinetic properties.

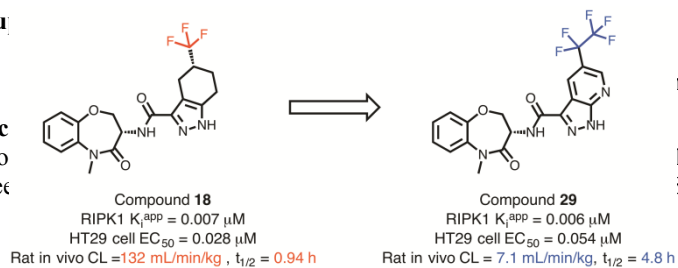
## Acknowledgments

We gratefully acknowledge support from the Genentech Discovery Chemistry Analytical and Purifications, Compound Management, and Protein Chemistry groups.

## References and notes

- Newton, K.; Manning, G. *Ann. Rev. Biochem.* **2016**, *85*, 743–763.
- Silke, J.; Rickard, J.A.; Gerlic, M. *Nat. Immunol.* **2015**, *16*, 689–697.
- Moriwaki, K.; Chan, F.K. *Cell. Mol. Life Sci.* **2016**, *73*, 2325–2334.
- Weinlich, R.; Oberst, A.; Beere, H. M.; Green, D. R. *Nat. Rev. Mol. Cell Biol.* **2017**, *18*, 127–136.
- Wegner, K. W.; Saleh, D.; Degterev, A. *Trends Pharmacol. Sci.* **2017**, *38*, 202–225.
- Linkermann, A.; Bräsen, J. H.; Himmerkus, N.; Liu, S.; Huber, T. B.; Kunzendorf, U.; Krautwald, S. *Kidney Int.* **2012**, *81*, 751–761.
- Degterev, A.; Huang, Z.; Boyce, M.; Li, Y.; Jagtap, P.; Mizushima, N.; Cuny, G. D.; Mitchison, T. J.; Moskowitz, M. A.; Yuan, J. *Nat. Chem. Biol.* **2005**, *1*, 112–119.
- Newton, K.; Dugger, D.L.; Maltzman, A.; Greve, J.M.; Hedehus, M.; Martin-McNulty, B.; Carano, R.A.; Cao, T.C.; van Bruggen, N.; Bernstein, L.; Lee, W.P.; Wu, X.; DeVoss, J.; Zhang, J.; Jeet, S.; Peng, I.; McKenzie, B.S.; Roose-Girma, M.; Caplazi, P.; Diehl, L.; Webster, J.D.; Vucic, D. *Cell Death Differ.* **2016**, *23*, 1565–1576.
- Koudstaal, S.; Oerlemans, M.I.; Van der Spoel, T.I.; Janssen, A.W.; Hoefler, I.E.; Doevendans, P.A.; Sluijter, J.P.; Chamuleau, S.A. *Eur. J. Clin. Invest.* **2015**, *45*, 150–159.
- Dannappel, M.; Vlantis, K.; Kumari, S.; Polykratis, A.; Kim, C.; Wachsmuth, L.; Eftychi, C.; Lin, J.; Corona, T.; Hermance, N.; Zelic, M.; Kirsch, P.; Basic, M.; Bleich, A.; Kelliher, M.; Pasparakis, M. *Nature* **2014**, *513*, 90–94.
- Takahashi, N.; Vereecke, L.; Bertrand, M. J. M.; Duprez, L.; Berger, S. B.; Divert, T.; Goncalves, A.; Sze, M.; Gilbert, B.; Kourula, S.; Goossens, V.; Lefebvre, S.; Gunther, C.; Becker, C.; Bertin, J.; Gough, P. J.; Declercq, W.; van Loo, G.; Vandenabeele, P. *Nature* **2014**, *513*, 95–99.
- Welz, P. S.; Wullaert, A.; Vlantis, K.; Kondylis, V.; Fernandez-Majada, V.; Ermolaeva, M.; Kirsch, P.; Sterner-Kock, A.; van Loo, G.; Pasparakis, M. *Nature* **2011**, *477*, 330–334.
- Weisel, K.; Scott, N. E.; Tompson, D. J.; Votta, B. J.; Madhavan, S.; Povey, K.; Wolstenholme, A.; Rudo, T.; Richards-Peterson, L.; Sahota, T.; Wang, J. G.; Lich, J.; Finger, J.; Verticelli, A.; Reilly, M.; Gough, P. J.; Harris, P. A.; Bertin, J.; Wang, M.-L. *Pharmacol. Res. Perspect.* **2017**, *5*, e00365, DOI: 10.1002/prp2.365
- Xie, T.; Peng, W.; Liu, Y.; Yan, C.; Maki, J.; Degterev, A.; Yuan, J.; Shi, Y. *Structure* **2013**, *21*, 493–499.
- Harris, P. A.; King, B. W.; Bandyopadhyay, D.; Berger, S. B.; Campobasso, N.; Capriotti, C. A.; Cox, J. A.; Dare, L.; Dong, X.; Finger, J. N.; Grady, L. C.; Hoffman, S. J.; Jeong, J. U.; Kang, J.; Kasparcova, V.; Lakdawala, A. S.; Lehr, R.; McNulty, D. E.; Nagilla, R.; Ouellette, M. T.; Pao, C. S.; Rendina, A. R.; Schaeffer, M. C.; Summerfield, J. D.; Swift, B. A.; Totoritis, R. D.; Ward, P.; Zhang, A.; Zhang, D.; Marquis, R. W.; Bertin, J.; Gough, P. J. *J. Med. Chem.* **2016**, *59*, 2163–2178.
- Harris, P. A.; Berger, S. B.; Jeong, J. U.; Nagilla, R.; Bandyopadhyay, D.; Campobasso, N.; Capriotti, C. A.; Cox, J. A.; Dare, L.; Dong, X.; Eidam, P. M.; Finger, J. N.; Hoffman, S. J.; Kang, J.; Kasparcova, V.; King, B. W.; Lehr, R.; Lan, Y.; Leister, L. K.; Lich, J. D.; MacDonald, T. T.; Miller, N. A.; Ouellette, M. T.; Pao, C. S.; Rahman, A.; Reilly, M. A.; Rendina, A. R.; Rivera, E. J.; Schaeffer, M. C.; Sehon, C. A.; Singhaus, R. R.; Sun, H. H.; Swift, B. A.; Totoritis, R. D.; Vossenkamper, A.; Ward, P.; Wisnoski, D. D.; Zhang, D.; Marquis, R. W.; Gough, P. J.; Bertin, J. *J. Med. Chem.* **2017**, *60*, 1247–1261.
- Berger, S. B.; Harris, P.; Nagilla, R.; Kasparcova, V.; Hoffman, S.; Swift, B.; Dare, L.; Schaeffer, M.; Capriotti, C.; Ouellette, M.; King, B. W.; Wisnoski, D.; Cox, J.; Reilly, M.; Marquis, R. W.; Bertin, J.; Gough, P. J. *Cell Death Dis.* **2015**, *1*, 15009.
- Ren, Y.; Su, Y.; Sun, L.; He, S.; Meng, L.; Liao, D.; Liu, X.; Ma, Y.; Liu, C.; Li, S.; Ruan, H.; Lei, X.; Wang, X.; Zhang, Z. *J. Med. Chem.* **2017**, *60*, 972–986.
- Yoshikawa, M.; Saitoh, M.; Katoh, T.; Seki, T.; Bigi, S.V.; Shimizu, Y.; Ishii, T.; Okai, T.; Kuno, M.; Hattori, H.; Watanabe, E.; Saikatendu, K.S.; Zou, H.; Nakakariya, M.; Tatamiya, T.; Nakada, Y.; Yogo, T. *J. Med. Chem.* **2018**, *61*, 2384–2409.
- Harris, P. A.; Bandyopadhyay, D.; Berger, S. B.; Campobasso, N.; Capriotti, C. A.; Cox, J. A.; Dare, L.; Finger, J. N.; Hoffman, S. J.; Kahler, K. M.; Lehr, R.; Lich, J. D.; Nagilla, R.; Nolte, R. T.; Ouellette, M. T.; Pao, C. S.; Schaeffer, M. C.; Smallwood, A.; Sun, H. H.; Swift, B. A.; Totoritis, R. D.; Ward, P.; Marquis, R. W.; Bertin, J.; Gough, P. J. *ACS Med. Chem. Lett.* **2013**, *4*, 1238–1243.
- (a) Lovering, F.; Bikker, J.; Humblet, C. *J. Med. Chem.* **2009**, *52*, 6752–6756. (b) Ritchie, T. J.; Macdonald, S. J.; Young, R. J.; Pickett, S. D. *Drug Discov. Today* **2011**, *16*, 164–71.
- Hopkins, A. L.; Groom, C. R.; Alex, A. *Drug Discov. Today* **2004**, *9*, 430–431.
- In vivo rat pharmacokinetic studies were conducted in male Sprague-Dawley rats; IV dosing at 0.5 mg/kg in 10% DMSO/60% PEG400/30% H<sub>2</sub>O vehicle (solution), PO dosing at 2 mg/kg in 10% DMSO/90% MCT (suspension). Data are the mean from three animals.
- Reviews on use of fluorinated motifs in medicinal chemistry: (a) Meanwell, N. A. *J. Med. Chem.* **2018**, *61*, 5822–5880. (b) Zhou, Y.; Wang, J.; Gu, Z.; Wang, S.; Zhu, W.; Aceña, J. L.; Soloshonok, V. A.; Izawa, K.; Liu, H. *Chem. Rev.* **2016**, *116*, 422–518.
- Reviews on fluoroalkyl cross-coupling: (a) Tomashenko, O. A.; Grushin, V. V. *Chem. Rev.* **2011**, *111*, 4475–4521. (b) Chen, P.; Liu, G. *Synthesis* **2013**, *45*, 2919–2939. (c) Alonso, C.; de Marigorta, E. M.; Rubiales, G.; Palacios, F. *Chem. Rev.* **2015**, *115*, 1847–1935
- Examples of pentafluoroethyl cross-coupling methods: (a) Mormino, M. G.; Fier, P. S.; Hartwig, J. F. *Org. Lett.* **2014**, *16*, 1744–1747. (b) Serizawa, H.; Aikawa, K.; Mikami, K. *Org. Lett.* **2014**, *16*, 3456–3459. (c) Aikawa, K.; Nakamura, Y.; Yokota, Y.; Toya, W.; Mikami, K. *Chem. Eur. J.* **2015**, *21*, 96–100. (d) Sugiishi, T.; Kawauchi, D.; Sato, M.; Sakai, T.; Amii, H. *Synthesis* **2017**, *49*, 1874–1878. (e) Li, L.; Ni, C.; Xie, Q.; Hu, M.; Wang, F.; Hu, J. *Angew. Chem. Int. Ed.* **2017**, *56*, 9971–9975. (f) Ferguson, D. M.; Bour, J. R.; Canty, A. J.; Kampf, J. W.; Sanford, M. S. *J. Am. Chem. Soc.* **2017**, *139*, 11662–11665.

Su

Ac  
Co  
bec

ie online version, at:

1 (1-294, C34A, C127A, C233A, C240A) and compound **11** have  
5NW2.

ACCEPTED MANUSCRIPT